ISSN: 2688-8645

The Release Kinetics of Long-Lasting Tracer Particles in Horizontal Wells

Zhaoyan Yue

School of Xi'an Shiyou University, Xi'an 710065, China

Abstract

In the context of China's ongoing development of unconventional oil and gas reservoirs, horizontal well segmental fracturing technology currently holds a dominant position. Accurate and effective monitoring of fracture parameters and production profiles is imperative for the efficient development of oil and gas resources. Tracer monitoring technology has emerged as a pivotal method for monitoring horizontal wells fractured in tight oil segments. This technology involves the injection of slow-release tracer particles into the fractured fracture, followed by the continuous monitoring of the tracer concentration during the fracture return period and the subsequent production process. The primary advantages of this approach include the ability to characterize fracture parameters of fractured fractures in tight oil horizontal wells and to monitor production profiles during normal production. This method provides a novel approach for real-time and cost-effective monitoring of the production dynamics of horizontal wells. Consequently, this study utilizes independently prepared samples of slow-release tracer particles to conduct an in-depth study of their release kinetic modeling on the basis of microscopic imaging observation. Microscopic observation revealed the existence of micropores, channels, and other structures within the long-acting tracer particles, which contributed to the stable release of the tracer active ingredient. The release kinetic model of the slow-release tracer particles demonstrates its capacity to approximately explain the release process of the tracer particles. The model also reveals that factors such as the diffusion coefficient, the solubility of the tracer components, the radius of the initial tracer components, and the mass of the tracer components per unit volume promote the release process. Conversely, the concentration of the solution to which the tracer particles are exposed has an inhibitory effect on the release process. The findings of this study establish a theoretical framework for the subsequent implementation of slow-release tracer particles in horizontal well fracturing and their comprehensive interpretation.

Keywords

Horizontal Wells; Segmented Fracturing; Slow-Release Tracer Particles.

1. Introduction

Horizontal well segmental fracturing technology has emerged as a pivotal element in the development of tight and shale oil. However, as the technology continues to evolve, the challenges associated with fracturing fracture awareness and the identification of water-seeing sections at the bottom of horizontal wells are becoming increasingly pronounced[1][2]. A comprehensive understanding of fracturing fractures is imperative for the optimization of fracturing parameters and production regimes. Consequently, the long-term reliable monitoring of fractured horizontal wells is paramount.

Compared with vertical wells, monitoring horizontal wells poses significant challenges due to complex fluid flow patterns, extensive borehole undulations, and heterogeneity.Current monitoring tools are limited in their effectiveness, including direct near-well monitoring (e.g., logging), direct far-field monitoring (e.g., microseismic), and indirect monitoring (e.g., pressure analysis)[3]. Each approach has inherent limitations. Distributed fiber-optic sensors, for instance, are costly and complex; microseismic monitoring cannot evaluate fluid seepage in the post-pressure fracture network; and net pressure fitting and well test analysis results rely on model assumptions and reservoir description accuracy.Tracers offer a unique advantage in monitoring fractured horizontal wells, as they can directly track fluid flow trajectories and visually indicate spatial properties. The technology for rejecting fracturing tracers has reached a relatively advanced stage, and the effect of each fracturing section is evaluated by adding tracers to different fracturing sections[4]. However, the existing technology mainly monitors the tracer output during the re-drainage period and is unable to track dynamic changes under long-term production. While intelligent tracer measurement of horizontal well fluid production profile technology can monitor long-term, it lacks the capacity to interpret and evaluate the fracturing effect of segments. This process is intricate and carries downhole risks.China's involvement in this field is recent, yet it has achieved successful development and application[5][6].

In light of the aforementioned limitations, this paper proposes the development of slow-release tracer particles that can be directly placed in fractured cracks and investigates their release kinetics in depth[7][8]. This will provide a reliable foundation for the implementation of long-term tracer monitoring, the optimization of fracturing processes, and water plugging in horizontal wells.Furthermore, this study is of significant importance in enhancing our understanding of the characteristics and principles governing water sighting in horizontal wells and expanding the application of tracers. By continuously improving and expanding tracer monitoring technology, a more scientific basis and reliable means for oil and gas field development will be provided[9][10].

2. Preparation of Long-Lasting Tracer Particles

The concept of skeleton type particles suggests that long-acting tracer particles utilize a polymer skeleton material to enclose the tracer active ingredient, thereby facilitating the gradual release of the internal active ingredient. This type of particle bears resemblance to slow-release long-acting drugs, wherein the tracer active ingredient is uniformly dispersed within the internal skeleton. This results in the external liquid's gradual infiltration into the internal space through minute pores. Consequently, the tracer ingredient can only diffuse to the external environment through the pores of the substrate skeleton, thereby achieving the long-acting effect.

The experiments in this paper utilize self-developed samples of long-lasting tracer particles, which are informed by the research findings on solid tracers. In the selection of raw materials for the tracer particles' skeleton, factors such as molecular structure, temperature resistance, cost-effectiveness, environmental impact, and other criteria pertinent to long-lasting tracer particles were considered. It was determined that the polymer material HS-N is well-suited for the fabrication of the tracer particles' skeleton as the substrate. The selection of tracer A and curing agent B as the active ingredients and compatible curing agents for the production of long-lasting tracer particles is predicated on the theory of long-lasting skeleton. Tracer A boasts the advantages of low cost, ease of procurement, and safety in use, rendering it well-suited for the preparation of samples. The mass ratio of the polymer material HS-N, tracer A, and curing agent B was selected as 10:3:5.6 for the preparation of long-lasting tracer particles. The mixture was thoroughly mixed and stirred, preheated for 15 minutes, and subsequently placed into a tubular mold with a diameter of 1 mm, length: 15 cm) and placed in an electric blast dryer at 90 °C for a heat treatment of 3.5 h. After the co-mixed material was cured into a cylindrical

ISSN: 2688-8645

shape, it was demolded and cut, and finally screened out the uniformly sized particles, which were then cut out. Following the curing of the co-mixture into a cylindrical shape, it was demolded and cut, and the particles of uniform size were subsequently screened for subsequent experiments (Fig. 1).

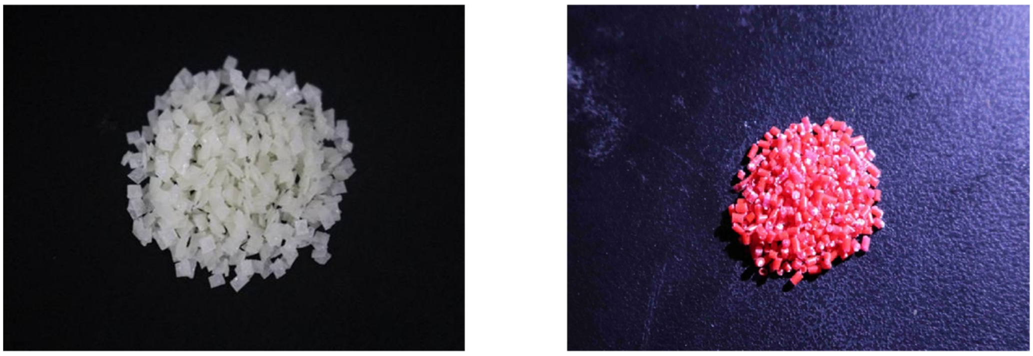

Fig 1. Samples of long-lasting tracer particles

Microscopic observation of the long-lasting tracer particle samples reveals the presence of a substantial number of small pores, micropores, and channels within the particles, as illustrated in Fig.2. These pores function as conduits for the diffusion of the active ingredients present within the long-lasting tracer particles from the interior to the exterior. Additionally, they serve as primary pathways for the ingress of active ingredients from the exterior into the interior during the process of being washed by external fluid.

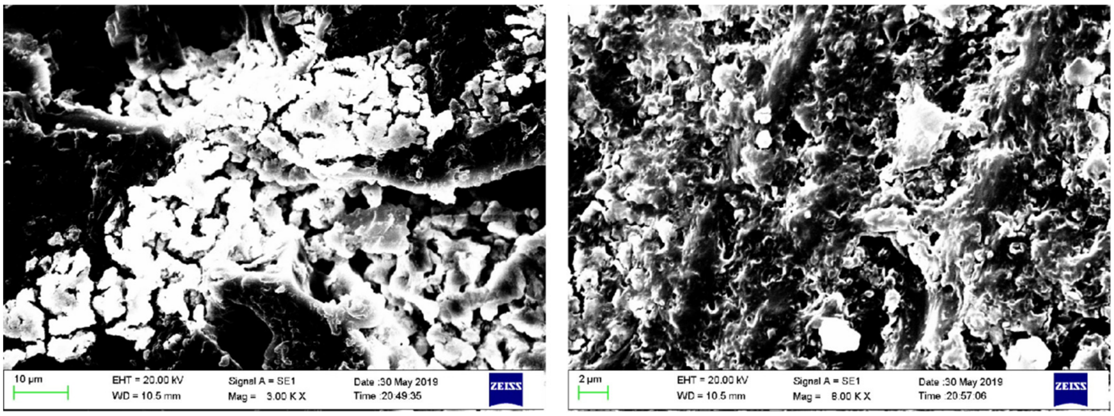

Fig 2. Microscopic images of long-lasting tracer particles

3. Modeling of Release Kinetics of Slow-Release Tracer Particles

3.1. The Release of Tracer Particles was Physically Modeled to Investigate the Release Mechanism of Slow-Release Particles

In light of the preceding experimental studies, it has been determined that the tracer components within the tracer particles can be gradually released to the external environment by leveraging the pore structure of the tracer particle skeleton. In conjunction with the theory of release of skeletal drugs, it is hypothesized that the release law of tracer particles is as follows: the tracer components inside the tracer particles are usually uniformly distributed in the basal skeleton of the tracer particles, and during the release process of the tracer particles, the solvent that penetrates into the internal part of the tracer particles The solvent gradually dissolves the uniformly distributed tracer components from the periphery to the internal part of the tracer particles. However, the solvent cannot rapidly dissolve the tracer components due to the substantial drug-carrying capacity of the tracer particles. Due to the substantial drug-loading capacity of the tracer particles, the solvent that penetrates the interior is unable to rapidly dissolve the tracer components in contact with it. Instead, the dissolution process is gradual and prolonged, resulting in the diffusion of the dissolved tracer components to the exterior via the pore crack structure of the basal skeleton, driven by the concentration gradient. As the tracer particles are released, an increasing number of tracer components are dissolved within them, leading to the formation of a distinct interface between the regions of the tracer particles that have been released and those that have not (Fig.3)[11][12].

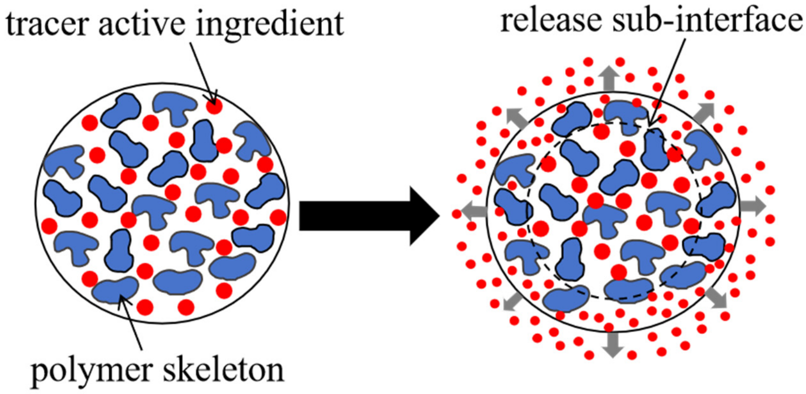

Fig 3. Tracer particle release process

In light of the comprehension regarding the release process of tracer particles, the subsequent physical model for the release of tracer particles has been formulated (Fig.4).

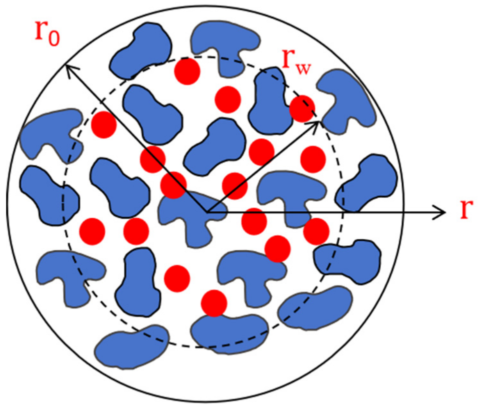

Fig 4. Tracer sphere release model (computing)

The fundamental assumptions of the model are as follows: the initial tracer component filling radius of the tracer particle is designated as r0, and the mass of the tracer component contained per unit volume of the tracer sphere particle is denoted by ρ. The movable boundary of the tracer particle is indicated by r_w, and the concentration gradient in the region of $r<r_w$ is defined as such. The concentration gradient in the region of $r<r_w$ is considered to be zero, and no release of the tracer component is distributed in the region. The change of concentration in the region of $r_w<r<r_0$ is regarded as a function of r. Furthermore, the diffusion of concentration in the region of $r_w<r<r_0$ is assumed to satisfy Fick's first law.

3.2. Mathematical Modeling of Slow-Release Tracer Particle Release

In the context of pseudo-steady-state conditions, the total amount of drug released per unit time, denoted by dt, is equal to dM. Concurrently, the change in the moving boundary within the tracer sphere per unit time, denoted by d-rw, is governed by Fick's first law:

$$\frac{dM}{dt} = -4r^2 \pi D \frac{dC}{dr} \tag{1}$$

Initial conditions are:

$r=r_0$, $C=C_0$

The boundary conditions are:

$r=r_w$, $C=C_s$

The preceding equation illustrates a mathematical model of tracer particle release.

The mass of the tracer component contained within a unit volume of the tracer sphere grain is denoted by ρ.

As demonstrated in Fig.4, the initial tracer component filling radius of the entire sphere, designated as r_0, and the moving boundary within the tracer sphere, denoted as r_w, are critical parameters. In such a system, the concentration gradient in the region $r<r_w$ is zero, and there is no release of the tracer component distributed in the region. The concentration change in the region $r_w<r<r_0$ can be considered as a function of r, and it is assumed that the concentration diffusion is in accordance with Fick's first law. Initial conditions were obtained with $C=C_0$ at $r=r_0$ and $C=C_s$ at $r=r_w$.

Integrating Eq. (1) from r_0 gives:

$$\left(\frac{dM}{dt}\right)_t \left(\frac{1}{r} - \frac{1}{r_0}\right) = 4\pi D(C - C_0) \tag{2}$$

The following equation is true when $r = r_w$.

$$\left(\frac{dM}{dt}\right)_t = \frac{4\pi D(C - C_0)}{\left(\frac{1}{r} - \frac{1}{r_0}\right)} = \frac{4\pi D(C_s - C_0)}{\left(\frac{1}{r_w} - \frac{1}{r_0}\right)} \tag{3}$$

Given the established relationships between C and r, namely C=C0 at $r=r_0$ and C=Cs at $r=r_w$, the subsequent relationship between r and the concentration C over the region rw<r<r0 can be deduced.

$$C = \frac{C_s - C_0}{r_0 - r_w} \cdot \frac{r_w r_0}{r} + \frac{C_0 r_0 - C_s r_w}{r_0 - r_w} \tag{4}$$

The tracer component residue of a tracer sphere at any given moment comprises the sum of the tracer components in the unreleased region ($r<r_w$) and in the released region ($r_w<r<r_0$), and its tracer component residue is defined as follows:

$$\begin{aligned} M_s &= \frac{4}{3} r_w^3 \pi\rho + \int_{r_w}^{r_0} 4\pi r^2 C dr \\ &= \frac{4}{3} r_w^3 \pi\rho + \int_{r_w}^{r_0} 4\pi r^2 \left(\frac{C_s - C_0}{r_0 - r_w} \cdot \frac{r_w r_0}{r} + \frac{C_0 r_0 - C_s r_w}{r_0 - r_w}\right) dr \\ &= \frac{4}{3} r_w^3 \pi\rho + 4\pi \int_{r_w}^{r_0} \left(\frac{C_s - C_0}{r_0 - r_w}\right) \cdot r_w r_0 r dr + 4\pi \int_{r_w}^{r_0} \left(\frac{C_0 r_0 - C_s r_w}{r_0 - r_w}\right) \cdot r^2 dr \\ &= \frac{4}{3} r_w^3 \pi\rho + 2\pi \left(\frac{C_s - C_0}{r_0 - r_w}\right) r_w r_0 \cdot \left(r_0^2 - r_w^2\right) + \frac{4}{3}\pi \left(\frac{C_0 r_0 - C_s r_w}{r_0 - r_w}\right) \cdot \left(r_0^3 - r_w^3\right) \\ &= \frac{4}{3} r_w^3 \pi\rho + 2\pi (C_s - C_0) \cdot \left(r_w r_0^2 + r_w^2 r_0\right) + \frac{4}{3}\pi \left(C_0 r_0 - C_s r_w\right) \cdot \left(r_0^2 + r_w r_0 + r_w^2\right) \end{aligned} \tag{5}$$

The variable can be obtained as a function of the tracer component residue and the movable boundary.

$$M_s(r_w)=\frac{4}{3}r_w^3\pi\rho+2\pi(C_s-C_0)\cdot(r_wr_0^2+r_w^2r_0)+\frac{4}{3}\pi(C_0r_0-C_sr_w)\cdot(r_0^2+r_wr_0+r_w^2) \tag{6}$$

The rate of change of its tracer component residue M_s with respect to the movable boundary r_w is:

$$\begin{aligned}\frac{\mathrm{d}M_s(r_w)}{\mathrm{d}(r_w)}&=4r_w^2\pi\rho+2\pi(C_s-C_0)\cdot(r_0^2+2r_wr_0)+\frac{4}{3}\pi(-C_s)(r_0^2+r_wr_0+r_w^2)+\frac{4}{3}\pi(C_0r_0-C_sr_w)\cdot(r_0+2r_w)\\&=4r_w^2\pi\rho+2\pi(C_s-C_0)\cdot(r_0^2+2r_wr_0)+\frac{4}{3}\pi\left[-C_sr_0^2-C_sr_wr_0-C_sr_w^2+C_0r_0^2+2C_0r_wr_0-C_sr_wr_0-2C_sr_w^2\right]\\&=4r_w^2\pi\rho+2\pi(C_s-C_0)\cdot(r_0^2+2r_wr_0)+\frac{4}{3}\pi\left[-C_sr_0^2-2C_sr_wr_0+2C_0r_wr_0+C_0r_0^2-3C_sr_w^2\right]\\&=4r_w^2\pi\rho+2\pi(C_s-C_0)\cdot(r_0^2+2r_wr_0)+\frac{4}{3}\pi(C_0-C_s)\cdot(r_0^2+2r_wr_0)-4\pi C_sr_w^2\\&=4r_w^2\pi\rho+\frac{2}{3}\pi(C_s-C_0)\cdot(r_0^2+2r_wr_0)-4\pi C_sr_w^2\end{aligned} \tag{7}$$

The alteration in the tracer component residue, Ms, is mathematically equivalent to the total drug released per unit time, yet it is oppositely directed. Consequently, the following equation is established:

$$\frac{4\pi D(C_s-C_0)}{\left(\frac{1}{r_w}-\frac{1}{r_0}\right)}\mathrm{d}t=\left[4r_w^2\pi\rho+\frac{2}{3}\pi(C_s-C_0)\cdot(r_0^2+2r_wr_0)-4\pi C_sr_w^2\right]\mathrm{d}(-r_w) \tag{8}$$

$$\begin{aligned}D\mathrm{d}t&=-\left\{\left(\frac{1}{r_w}-\frac{1}{r_0}\right)\cdot\frac{1}{(C_s-C_0)}\left[r_w^2\rho+\frac{1}{6}(C_s-C_0)\cdot(r_0^2+2r_wr_0)-C_sr_w^2\right]\right\}\mathrm{d}r_w\\&=-\left[\left(\frac{1}{r_w}-\frac{1}{r_0}\right)\cdot\frac{(\rho-C_s)r_w^2}{(C_s-C_0)}+\frac{1}{6}\left(\frac{1}{r_w}-\frac{1}{r_0}\right)\cdot(r_0^2+2r_wr_0)\right]\mathrm{d}r_w\\&=-\left[\frac{(\rho-C_s)r_w}{(C_s-C_0)}-\frac{(\rho-C_s)r_w^2}{(C_s-C_0)}\cdot\frac{1}{r_0}+\frac{1}{6}\left(\frac{r_0^2}{r_w}+r_0-2r_w\right)\right]\mathrm{d}r_w\end{aligned} \tag{9}$$

The temporal variable t integrates from the initial value r0 to the final value r_w .

$$\int_0^t D\mathrm{d}t=-\int_{r_0}^{r_w}\left[\frac{(\rho-C_s)r_w}{(C_s-C_0)}-\frac{(\rho-C_s)r_w^2}{(C_s-C_0)}\cdot\frac{1}{r_0}+\frac{1}{6}\left(\frac{r_0^2}{r_w}+r_0-2r_w\right)\right]\mathrm{d}r_w \tag{10}$$

Available:

$$\begin{aligned}6Dt&=\frac{3(C_s-\rho)}{(C_s-C_0)}(r_w^2-r_0^2)-\frac{2(C_s-\rho)}{(C_s-C_0)}\cdot(r_w^3-r_0^3)\frac{1}{r_0}-\left(r_0^2\cdot In\left(\frac{r_w}{r_0}\right)+r_0r_w-r_w^2\right)\\&=\frac{(C_s-\rho)}{(C_s-C_0)}\left[3(r_w^2-r_0^2)-2(r_w^3-r_0^3)\frac{1}{r_0}\right]-\left(r_0^2\cdot In\left(\frac{r_w}{r_0}\right)+r_0r_w-r_w^2)\right)\\&=\frac{(C_s-\rho)}{(C_s-C_0)}\left[3r_w^2-2\frac{r_w^3}{r_0}-r_0^2\right]-\left(r_0^2\cdot In\left(\frac{r_w}{r_0}\right)+r_0r_w-r_w^2)\right)\end{aligned} \tag{11}$$

Therefore, the relationship between the moving boundary r_w and time t can be obtained.

$$6Dr_0t=\frac{(C_s-\rho)}{(C_s-C_0)}\left[3r_w^2r_0-2r_w^3-r_0^3\right]+\left(r_0^3\cdot In\left(\frac{r_0}{r_w}\right)-r_0^2r_w+r_w^2r_0\right) \tag{12}$$

Cumulative release of tracer particles:

$$\begin{aligned}M_t&=\frac{4}{3}\rho\pi(r_0^3-r_w^3)-\int_{r_w}^{r_0}4\pi r^2Cdr\\&=\frac{4}{3}\rho\pi(r_0^3-r_w^3)-2\pi(C_s-C_0)\cdot\left(r_wr_0^2+r_w^2r_0\right)-\frac{4}{3}\pi\left(C_0r_0-C_sr_w\right)\cdot\left(r_0^2+r_wr_0+r_w^2\right)\end{aligned} \tag{13}$$

Equation (13) represents the analytical solution of the release model of the slow-release tracer particles (single sphere). This formula can provide a theoretical model basis for the subsequent establishment of multiple slow-release tracer particles release models, thereby clarifying its slow-release law.

4. Basic Curve Analysis of the Release of Slow-Release Tracer Particles

4.1. The Release of Tracer Particles was Physically Modeled to Investigate the Release Mechanism of Slow-Release Particles.

The release kinetics of slow-release tracer particles (single spheres) were modeled as follows:

$$\begin{cases}6Dr_0t=\dfrac{(C_s-\rho)}{(C_s-C_0)}\left[3r_w^2r_0-2r_w^3-r_0^3\right]+\left(r_0^3\cdot In\left(\dfrac{r_0}{r_w}\right)-r_0^2r_w+r_w^2r_0\right)\\M_t=\dfrac{4}{3}\rho\pi(r_0^3-r_w^3)-2\pi\left(C_s-C_0\right)\cdot\left(r_wr_0^2+r_w^2r_0\right)-\dfrac{4}{3}\pi\left(C_0r_0-C_sr_w\right)\cdot\left(r_0^2+r_wr_0+r_w^2\right)\end{cases} \tag{14}$$

included among these:

D:Diffusion coefficient of the tracer component inside the tracer particle, cm2/s; r_0:Radius of initial tracer component of tracer particles, cm; t:Tracer particle release time,s; C_s:Tracer component solubility,g/cm3; ρ:Mass of tracer component contained per unit volume, g/cm^3; C_0:Concentration of the solution to which the tracer particles are exposed, g/cm^3; r_w:The interface between the released and unreleased regions of the tracer particles, cm; M_t:Cumulative mass released from the tracer particles, g.

The initial step entails the configuration of the model parameters in the following manner:

Table 1. Tracer particle release kinetic model parameters

Mass of tracer component per unit volume(g/cm^3)	tracer component solubility(g/cm^3)	radius of tracer particle(cm)	diffusion coefficient(cm^2/s)	External Boundary Concentration(g/cm^3)
2.0	1.0	0.1	0.0001	0

In accordance with the aforementioned parameters, the movable boundary r_w and the cumulative release of the tracer component Mt with time were plotted as demonstrated in the following figure.

As demonstrated by the curve depicting the movable boundary's temporal progression, the movable radius undergoes a gradual decrease over time, signifying the progressive dissolution of tracer particles into the system's interior. The decline in the movable boundary's velocity indicates a reduction in the rate at which tracer particles are released. The analysis of the cumulative release curve of tracer components reveals a decline in the rate of increase of this curve, suggesting a slower rate of release. This finding indirectly suggests a decrease in the rate of tracer component release, which is consistent with the observed decline in the movable radius over time. A comparison of the cumulative release curves from the experimental tracer release reveals a general similarity in trend with the model curve, thereby suggesting the potential of the model to provide a reasonable explanation for the release process of tracer particles.

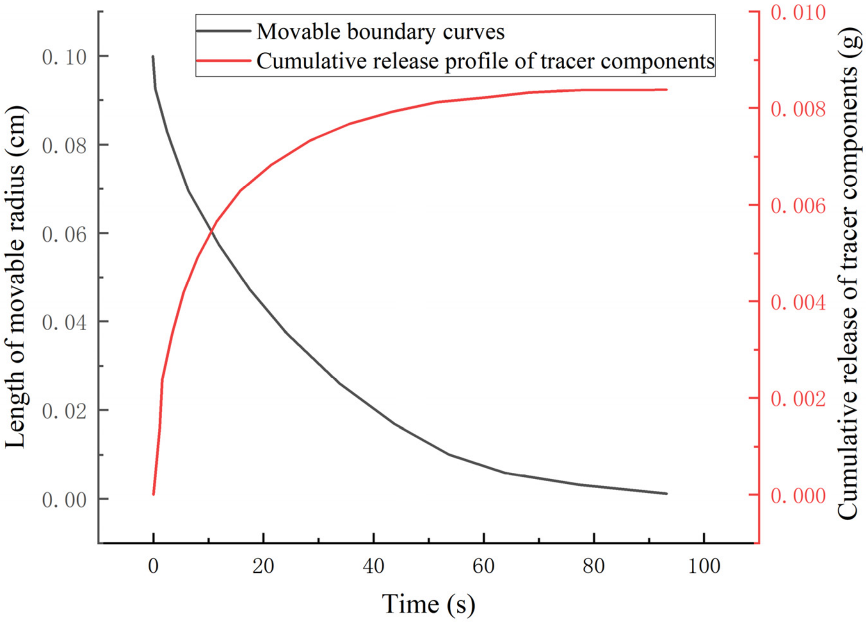

Fig 5. The following investigation will examine the cumulative release profiles of movable boundary and tracer components as a function of time.

4.2. Multiple Slow-Release Tracer Particle Release Profiles

The relevant parameters of the modeled release of multiple slow-release tracer particles are as follows:

Table 2. Parameters related to release modeling for each slow-release tracer particle

	Mass of tracer component per unit volume (g/cm³)	tracer component solubility (g/cm³)	radius of tracer particle (cm)	diffusion coefficient (cm²/s)	External Boundary Concentration (g/cm³)	Cumulative mass released (g)	Length of movable boundary (cm)
Particle 1	ρ	C_s	r_0	D	C_0	M_{t1}	r_{w1}
Particle 2						M_{t2}	r_{w2}
Particle 3						M_{t3}	r_{w3}
...						...	...
Particle n						M_{tn}	r_{wn}

The release kinetic model of single slow-release tracer particles was developed. This model is based on the assumption that the release concentration of all particles (spheres) is the same. The release concentration of each sphere is superimposed, and a transient interpretation model of the horizontal well of the smart tracer corresponding to it is established. This model is used

ISSN: 2688-8645

as a basis to explore the release law of the output curve of the active ingredient of multiple slow-release tracer particles.

The interpretation method principally utilizes the release model of each slow-release tracer particle for superposition processing. This process simplifies the interpretation model, facilitating interpretation and data fitting. The release kinetic model of single (single sphere) slow-release tracer particles has been established, and the corresponding release kinetic model of multiple particles can be obtained.

Particle 1 release model:

$$\begin{cases} 6Dr_0 t = \dfrac{(C_s-\rho)}{(C_s-C_0)}\left[3r_{w1}^2 r_0 - 2r_{w1}^3 - r_0^3\right] + \left(r_0^3 \cdot In\left(\dfrac{r_0}{r_{w1}}\right) - r_0^2 r_{w1} + r_{w1}^2 r_0\right) \\ M_{t1} = \dfrac{4}{3}\rho\pi(r_0^3 - r_{w1}^3) - 2\pi\left(C_s - C_0\right)\cdot\left(r_{w1}r_0^2 + r_{w1}^2 r_0\right) - \dfrac{4}{3}\pi\left(C_0 r_0 - C_s r_{w1}\right)\cdot\left(r_0^2 + r_{w1}r_0 + r_{w1}^2\right) \end{cases} \tag{15}$$

Particle 2 release model:

$$\begin{cases} 6Dr_0 t = \dfrac{(C_s-\rho)}{(C_s-C_0)}\left[3r_{w2}^2 r_0 - 2r_{w2}^3 - r_0^3\right] + \left(r_0^3 \cdot In\left(\dfrac{r_0}{r_{w2}}\right) - r_0^2 r_{w2} + r_{w2}^2 r_0\right) \\ M_{t2} = \dfrac{4}{3}\rho\pi(r_0^3 - r_{w2}^3) - 2\pi\left(C_s - C_0\right)\cdot\left(r_{w2}r_0^2 + r_{w2}^2 r_0\right) - \dfrac{4}{3}\pi\left(C_0 r_0 - C_s r_{w2}\right)\cdot\left(r_0^2 + r_{w2}r_0 + r_{w2}^2\right) \end{cases} \tag{16}$$

Particle 3 release model:

$$\begin{cases} 6Dr_0 t = \dfrac{(C_s-\rho)}{(C_s-C_0)}\left[3r_{w3}^2 r_0 - 2r_{w3}^3 - r_0^3\right] + \left(r_0^3 \cdot In\left(\dfrac{r_0}{r_{w3}}\right) - r_0^2 r_{w3} + r_{w3}^2 r_0\right) \\ M_{t3} = \dfrac{4}{3}\rho\pi(r_0^3 - r_{w3}^3) - 2\pi\left(C_s - C_0\right)\cdot\left(r_{w3}r_0^2 + r_{w3}^2 r_0\right) - \dfrac{4}{3}\pi\left(C_0 r_0 - C_s r_{w3}\right)\cdot\left(r_0^2 + r_{w3}r_0 + r_{w3}^2\right) \end{cases} \tag{17}$$

The particle n release model is defined by the following parameters: n represents the number of slow-release tracer particles, which are taken to be positive integers.

$$\begin{cases} 6Dr_0 t = \dfrac{(C_s-\rho)}{(C_s-C_0)}\left[3r_{wn}^2 r_0 - 2r_{wn}^3 - r_0^3\right] + \left(r_0^3 \cdot In\left(\dfrac{r_0}{r_{wn}}\right) - r_0^2 r_{wn} + r_{wn}^2 r_0\right) \\ M_{tn} = \dfrac{4}{3}\rho\pi(r_0^3 - r_{wn}^3) - 2\pi\left(C_s - C_0\right)\cdot\left(r_{wn}r_0^2 + r_{wn}^2 r_0\right) - \dfrac{4}{3}\pi\left(C_0 r_0 - C_s r_{wn}\right)\cdot\left(r_0^2 + r_{wn}r_0 + r_{wn}^2\right) \end{cases} \tag{18}$$

The release models corresponding to particles 1 through n are superimposed, and the results of this superposition are as follows:

$$\begin{cases} r_{w1} = r_{w2} = r_{w3} \ldots = r_{\mathrm{wn}} \\ M_{t总} = M_{t1} + M_{t2} + M_{t3} \ldots + M_{\mathrm{tn}} = \sum M_{tn} \end{cases} \tag{19}$$

included among these:

D: Diffusion coefficient of the tracer component inside the tracer particle, cm^2/s;

R_0:Radius of the initial tracer component of the tracer particle, cm;

t:Tracer particle release time, s;

C_s: Tracer component solubility, g/cm^3;

ρ: mass of tracer component contained per unit volume, g/cm^3;

C_0: concentration of the solution to which the tracer particles are exposed, g/cm^3;

r_{wn}: Interface between the released and unreleased regions of the tracer particle n, cm;

M_{tn}: Cumulative released mass of tracer particle n, g.

Equation (19) represents the release kinetic interpretation model corresponding to multiple particles. The relevant setup parameters of the model can be referred to Table 3. Utilizing the aforementioned parameters, the movable boundary rw of multiple slow-release tracer particles was plotted as a curve over time. Due to the uniform structure and tracer composition between the slow-release tracer particles. The tracer composition variation curve of cumulative release Mt with time is depicted in Fig.6.

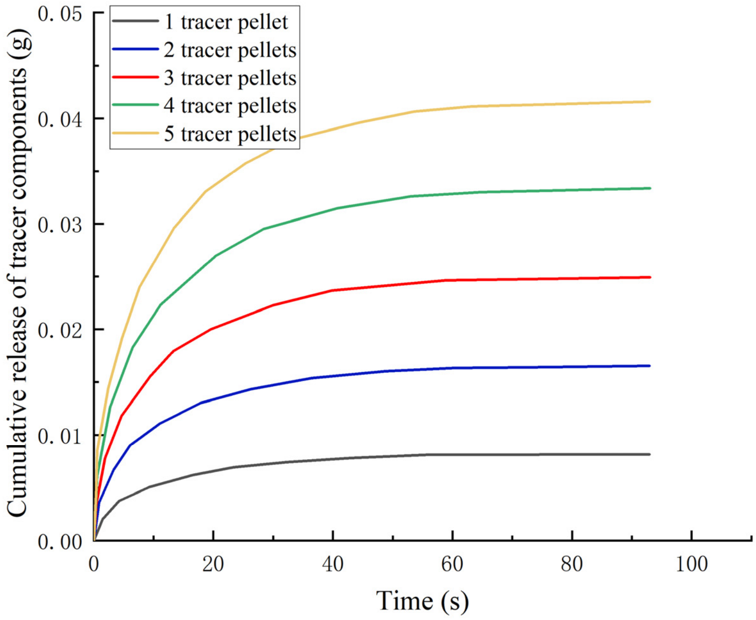

Fig 6. The following investigation will examine the cumulative release profile of tracer components from multiple slow-release tracer particles.

The cumulative release curves of tracer components of multiple slow-release tracer particles (Fig.6) demonstrate a clear trend of increasing cumulative release of tracer components with an increase in the number of slow-release tracer particles. The release of tracer components increased significantly and gradually stabilized. The model curves exhibited a high degree of similarity with the cumulative release curves of the release experiments, suggesting that the model can be used to approximate the release process of tracer particles. With an increase in the number of slow-release tracer particles, the time taken for the release to stabilize was longer, which indirectly indicated that the slow-release effect of the tracer component was more obvious, and the length of the slow-release time was related to the amount of tracer particles.

5. Summary

static slow-release kinetic experiments on slow-release tracer particles revealed the existence of pore, throat and other channel structures within the tracer particles, thereby enabling stable diffusion of the tracer active ingredient. Furthermore, it was observed that the instantaneous concentration curve exhibited rapid changes in the initial stage and gradual decline over time, aligning with the law of slow-release particles. The release kinetic models of single and multiple slow-release tracer particles were established and solved based on the release experiments of slow-release tracer particles and the theory of slow-release of insoluble skeleton drugs. The trend of the cumulative release curves was found to be roughly the same as that of the release experiments, which indicated that the model could be used to explain the release process of the tracer particles in a close approximation.

ISSN: 2688-8645

References

[1] Zou, C.N., Yang, Z., Zhu, R.K., et al. (2015). Advances in exploration, development, and theoretical technologies of unconventional hydrocarbons in China. Acta Geologica Sinica, 89(06), 979-1007.

[2] Guo, J.C., Ma, L., & Lu, C. (2022). Progress and development direction of fracturing and oil displacement technology in tight oil reservoirs in China. Acta Petrolei Sinica, 43(12), 1788-1797.

[3] Lei, Q., Xu, Y., Cai, B., et al. (2022). Progress and prospect of shale oil and gas horizontal well fracturing technology. Petroleum Exploration and Development, 49(01), 166-172+182.

[4] Li, D.J., Zhu, H.Z., Ma, G.W., Yang, H.T., & Du, X.Q. (2021). Current status of water detection technology in horizontal wells and discussion on rapid water detection methods. Petroleum Geology & Engineering, 35(01), 109-112+117.

[5] Liu, J.F. (2022). Progress and prospect of production profile testing technology for staged fracturing of horizontal wells. Special Oil & Gas Reservoirs, 29(05), 1-8.

[6] Li, H.T., Luo, H.W., Xiang, Y.H., et al. (2021). DTS-based artificial fracture identification and production profile interpretation method for shale gas horizontal wells. Natural Gas Industry, 41(05), 66-75.

[7] Sui, W.B., Liu, R.Q., & Cui, K. (2021). Application and research progress of distributed optical fiber acoustic sensing monitoring in hydraulic fracturing. Science China Technological Sciences, 51(04), 371-387.

[8] Sui, W.B., Zhang, D., Wang, M.Y., & Wang, X.Y. (2020). Application and theoretical model research progress of intelligent well temperature monitoring technology in oil and gas field development. Petroleum Geology and Recovery Efficiency, 27(03), 129-138.

[9] Liang, X.L., Liu, H.L., Cheng, N., & Zhang, R.L. (2021). Research and application of microseismic monitoring interpretation technology in unconventional oil and gas reservoirs. Xinjiang Oil & Gas, 17(03), 53-58.

[10] Liang, B.Y., Shen, C., Leng, C.B., et al. (2015). Research progress on microseismic fracturing monitoring technology. Progress in Geophysics, 30(01), 401-410.

[11] Zhang, F.Y., Zou, L.J., Cui, W., et al. (2022). Inversion method of fracture parameters in shale reservoirs based on fracturing fluid flowback data. Journal of Northeast Petroleum University, 46(01), 76-87+10.

[12] Jing, J.Y., Liu, C.L., Lan, X.T., et al. (2022). Research and application of seepage flow pattern analysis in fracture diagnosis of tight reservoirs. Fault-Block Oil & Gas Field, 29(03), 307-312.